Solid State Communications 146 (2008) 506–509

Contents lists available at ScienceDirect

Solid State Communications

journal homepage: www.elsevier.com/locate/ssc

Wide-angle, broadband plate polarizer in Terahertz frequency region

Suneet Kumar Awasthi [a,*], Anchal Srivastava [b], U. Malaviya [b], S.P. Ojha [c]

[a] *Amity Institute of Applied Science, Amity University, Noida-201301, India*
[b] *Department of Physics, University of Lucknow, Lucknow-226007, India*
[c] *Chaudhary Charan Singh University, Meerut-25004, India*

ARTICLE INFO

Article history:
Received 25 October 2007
Received in revised form
28 February 2008
Accepted 10 March 2008 by R.T. Phillips
Available online 18 March 2008

PACS:
78.67-n
94.20.ws

Keywords:
A. Multilayers
A. Thin films
D. Optical properties
D. Polarization

ABSTRACT

In this paper, a plate polarizer for use in the terahertz (THz) frequency region (0.10 THz to 0.15 THz) has been suggested. The polarizer which is effective over a wide range of angles of the incident light (angular field = 16°), is composed of thin film layers of silicon and air arranged alternately to form a stack. Here we show that the polarizer has a high performance in transmission, with maximum and minimum values of the degree of polarization given by 0.9999 and 0.9963 respectively. The polarizer has some advantages over the wide angle cube polarizers investigated earlier. Firstly, in the former, the total number of thin film layers is eleven, whereas in the latter, a larger number of thin film layers are cemented between the two prisms constituting a glass cube. The fabrication of cube polarizers is therefore an expensive procedure. Secondly, prisms exhibit stress related birefringence that changes with temperature and causes problems in imaging projectors. The proposed polarizer is free from such effects.

1. Introduction

Over the past decade, there has been a staggering increase in the number of research groups worldwide seeking to develop and exploit the terahertz frequency region, which spans from approximately 100 GHz to 10 THz [1]. This region has become a popular domain in spectroscopy and imaging [2–7]. Terahertz polarization-sensitive spectroscopy such as vibrational circular dichroism (VCD) spectroscopy is a new technique which has substantial potential in the fields of macromolecular chemistry and structural biology [6]. Hirota et al. [4] have fabricated a circular-polarization modulator of broadband THz radiation, which consisted of a four-contact photoconductive antenna and a Si prism, intended to realize the VCD spectrometer in THz frequency region, based on THz time domain spectroscopy. A three-contact photoconductive receiver, useful for VCD spectroscopy and ellipsometry in the THz frequency region was fabricated by Makabe et al. [2]. An ion-implanted InP receiver for polarization resolved THz spectroscopy was fabricated by Castro-Camus et al. [3].

Polarizers and polarizing beam splitters have not received much attention in the THz regime, although investigations in other frequency regions have been done [8–14]. In this communication, we have suggested a broadband plate polarizer for use in the terahertz frequency range (0.10 THz to 0.15 THz). The polarizer is effective over a wide range of angles of the incident light, with an angular field of 16°. Wide-angle, broadband polarizing beam splitters investigated earlier [8,12,13] were cube polarizers, in each of which, multilayers were cemented between the two prisms constituting a glass cube. Prisms exhibit stress-related birefringence that changes with temperature and causes problems in imaging projectors [15]. Moreover, these polarizers are expensive. So the need arises for a simple plate polarizer that could have a reasonably wide angular field and a reasonably large frequency range of operation. But, plate polarizers reported in literature have a small angular field and do not operate over a wide frequency range.

The proposed plate polarizer is composed of thin film layers of silicon and air arranged alternately to form a stack. The total number of layers is eleven. The structure may resemble the one described earlier in Reference [16], where high-purity silicon wafers were placed on silicon spacers to produce air gaps between them. The proposed structure is simpler compared to that of wide angle cube polarizers, where a large number of thin film layers were cemented between the two prisms. This number ranged from 22 to 81 as mentioned in References [8,12,13]. Thus fabrication of cube polarizers was an expensive procedure.

* Corresponding author. Tel.: +91 9212651231; fax: +91 0522 2202924.
E-mail address: suneet_electronic@yahoo.com (S.K. Awasthi).

0038-1098/$ – see front matter © 2008 Elsevier Ltd. All rights reserved.
doi:10.1016/j.ssc.2008.03.016

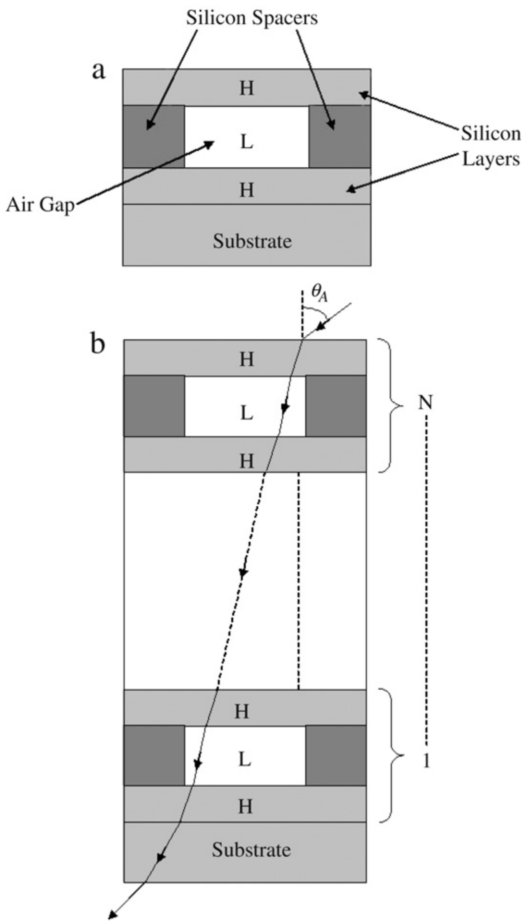

Fig. 1. Depiction of a one-dimensional *HLH* periodic lattice. (a) Basic structure (b) Structure with *N* periods.

In Section 2, the theoretical analysis upon which the study is based is presented. The mathematical formulation uses a transfer matrix method (TMM) [17,18]. Results obtained are presented in Section 3. Section 4 summarizes the results obtained.

2. Theoretical analysis

A three layer periodic thin film structure $n_A \left|[HLH]^N\right| n_S$ is taken, where H and L represent two different material layers with refractive indices n_H (higher) and n_L (lower), respectively, and N is the number of periods of the basic structure $[HLH]$. n_A is the refractive index of the incidence medium, which in this case is air, and n_s the refractive index of the semi-infinite medium at the exit end of the multilayer (Fig. 1).

The characteristic matrix for an N period structure is given by [17]

$$[M(d)]^N = \begin{bmatrix} M_{11}U_{N-1}(a) - U_{N-2}(a) & M_{12}U_{N-1}(a) \\ M_{21}U_{N-1}(a) & M_{22}U_{N-1}(a) - U_{N-2}(a) \end{bmatrix} \equiv \begin{bmatrix} m_{11} & m_{12} \\ m_{21} & m_{22} \end{bmatrix} \quad (1)$$

where

$$M_{11} = \left(\cos\gamma_1\cos\gamma_2\cos\gamma_3 - \frac{p_2}{p_1}\sin\gamma_1\sin\gamma_2\cos\gamma_3 - \frac{p_1}{p_2}\cos\gamma_1\sin\gamma_2\sin\gamma_3 - \sin\gamma_1\cos\gamma_2\sin\gamma_3\right),$$

$$M_{12} = -\mathrm{i}\left(\frac{1}{p_1}\sin\gamma_1\cos\gamma_2\cos\gamma_3 + \frac{1}{p_2}\cos\gamma_1\sin\gamma_2\cos\gamma_3 + \frac{1}{p_1}\cos\gamma_1\cos\gamma_2\sin\gamma_3 - \frac{p_2}{p_1^2}\sin\gamma_1\sin\gamma_2\sin\gamma_3\right),$$

$$M_{21} = -\mathrm{i}\left(p_1\sin\gamma_1\cos\gamma_2\cos\gamma_3 + p_2\cos\gamma_1\sin\gamma_2\cos\gamma_3 + p_1\cos\gamma_1\cos\gamma_2\sin\gamma_3 - \frac{p_1^2}{p_2}\sin\gamma_1\sin\gamma_2\sin\gamma_3\right),$$

$$M_{22} = \left(\cos\gamma_1\cos\gamma_2\cos\gamma_3 - \frac{p_1}{p_2}\sin\gamma_1\sin\gamma_2\cos\gamma_3 - \frac{p_2}{p_1}\cos\gamma_1\sin\gamma_2\sin\gamma_3 - \sin\gamma_1\cos\gamma_2\sin\gamma_3\right),$$

Here $\gamma = \frac{2\pi\nu}{c} nd\cos\theta$, θ is the ray angle inside the layer of refractive index n and thickness d, and is related to the angle of incidence θ_A by

$$\cos\theta = \left[1 - \frac{n_A^2\sin^2\theta_A}{n^2}\right]^{1/2}$$

ν is the frequency of the incident light wave, and c is the velocity of light in vacuum. The subscripts 1, 2 and 3 refer to the layers *HLH*, respectively.

$$\text{For s-polarization} \quad p = n\cos\theta \quad (2)$$

$$\text{For p-polarization} \quad p = \frac{\cos\theta}{n} \quad (3)$$

U_N are the Chebyshev polynomials of the second kind

$$U_N(a) = \frac{\sin[(N+1)\cos^{-1} a]}{[1-a^2]^{1/2}} \quad (4)$$

where

$$a = \frac{1}{2}[M_{11} + M_{22}], \quad (5)$$

The transmission coefficient of the multilayer is given by

$$t = \frac{T}{A} = \frac{2p_A}{(m_{11} + m_{12}p_S)p_A + (m_{21} + m_{22}p_S)} \quad (6)$$

The reflection coefficient of the multilayer is given by

$$r = \frac{R}{A} = \frac{(m_{11} + m_{12}p_S)p_A - (m_{21} + m_{22}p_S)}{(m_{11} + m_{12}p_S)p_A + (m_{21} + m_{22}p_S)} \quad (7)$$

where for s-polarization

$$p_A = n_A\cos\theta_A, \qquad p_S = n_S\cos\theta_S = n_S\left[1 - \frac{n_A^2\sin^2\theta_A}{n_S^2}\right]^{1/2} \quad (8)$$

and for p-polarization

$$p_A = \frac{\cos\theta_A}{n_A}, \qquad p_S = \frac{\cos\theta_S}{n_S} = \frac{\left[1 - \frac{n_A^2\sin^2\theta_A}{n_S^2}\right]^{1/2}}{n_S} \quad (9)$$

The subscript s refers to the medium of refractive index n_s. A, T and R are the amplitudes of the electric vectors of the incident, transmitted and reflected waves, respectively.

The transmissivity and reflectivity of the multilayer are given by

$$T = \frac{p_S}{p_A}|t|^2 \quad (10)$$

$$\Re = |r|^2 = rr^*. \quad (11)$$

3. Results and discussion

The high and low index layers shown in Fig. 1 are those of silicon and air, respectively. Silicon has been chosen because it has a high index of refraction in the region of investigation ($n_H = 3.4$) [19]. The low index layer has been taken to be that of air ($n_L = 1.0$) to further minimize losses. Thus a high index ratio ($n_H/n_L = 3.4$) is achieved giving a large frequency range of maximum reflectivity for s-polarized light. The refractive index of the exit medium is $n_S = 3.4$.

The Brewster angle condition for the structure is

$$\sin\theta_A = \frac{n_H}{\sqrt{1+n_H^2}} \tag{12}$$

When this condition is fulfilled, the s-polarized light will be reflected and the p-polarized light will be transmitted. For the materials selected, (silicon and air), condition (12) will be fulfilled at Brewster angle $73^\circ 36' 37''$. The lattice period (Λ) is taken to be equal to 625 µm. For each choice of n_H and n_L, there is a particular value of the filling fraction ($= d_L/\Lambda$) which gives maximum angular field of the polarizer. d_L is the thickness of the air gap. The optimum filling fraction η_{opt} corresponding to maximum angular field was numerically computed to be equal to 0.68, corresponding to which d_L was calculated to be equal to 425 µm. The silicon layers on either side of the air gap in one period of the ternary structure were taken to be equal to each other (=100 µm). The number of periods N, of the structure was optimized to give maximum reflectivity of the s-polarized component for the range of angles studied. N_{opt} was numerically computed to be equal to 5. This means a total of 11 layers.

Using expressions (1)–(10) the transmissivity spectra for the p and s polarized waves were plotted for angles of incidence equal to 64°, 69°, 74° and 80° (Figs. 2a and 2b). It is seen that the transmissivity of the s-polarized wave has a maximum value of 1.837×10^{-3} and a minimum value of 1.157×10^{-7} while that of the p-polarized wave varies between a minimum of 0.866 and a maximum of 1. It is therefore inferred that there is negligible transmittance of the s-polarized wave, but high transmittance of the p-polarized wave. However, for angles of incidence less than 64° and greater than 80°, the transmittance of the p-polarized wave decreases. The angle of incidence, therefore, limits the transmittance of the p-polarized component for the given frequency range. It is worth mentioning that the limitations on incidence angle can be overcome to a large extent if the lower edge of the given frequency range is increased, and its upper edge is decreased, thereby causing a decrease in the frequency range of operation of the polarizer.

Using expressions (1)–(9) and (11), the reflectivity spectra for the s and p polarized waves were determined for the same frequency range and for the same range of incidence angles. It is seen that the reflectivity of the s polarized light is ~1.0, while that of the p polarized component varies between a minimum of 2.068×10^{-8} and a maximum of 0.134. This indicates that the s-polarized wave which is almost absent in transmission, appears in reflection. The proposed polarizer is, therefore, a filter for the p-component. It is further noticed that, in the reflected light, a small amount of the p-component is also present. Since the maximum reflectivity of the p-component is 0.134, hence the device cannot be considered to be a good polarizing filter for the s-component in reflection.

In transmission, the degree of polarization is defined by [8]

$$P_T = \left|\frac{T_P - T_S}{T_P + T_S}\right|$$

where T_P, T_S are the transmittances for p- and s-polarized light, respectively. The maximum and minimum values of P_T for the range of frequencies and angles investigated were calculated to be equal to 0.9999 and 0.9963, respectively (Fig. 3). This indicates that the transmittance of the s-polarized wave can be considered to be negligible in comparison to that of the p-polarized component.

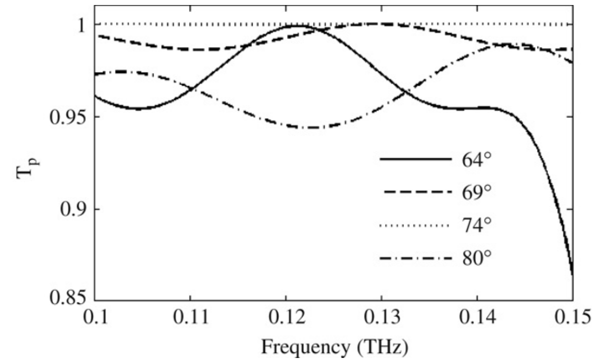

Fig. 2a. Transmissivity spectra of p-polarized wave for a 5 period Si/Air/Si structure with layer thicknesses 100/425/100 µm at angles of incidence equal to 64°, 69°, 74° and 80°. Maximum and minimum transmissivities are 1 and 0.866, respectively.

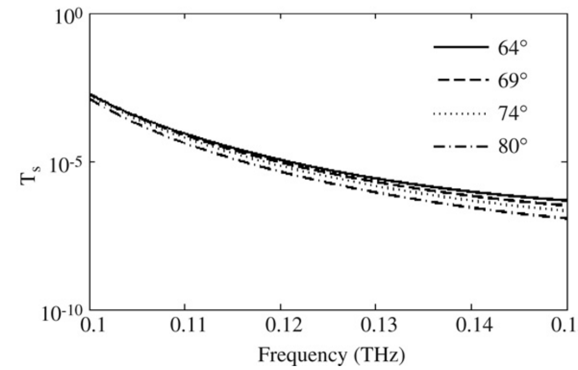

Fig. 2b. Transmissivity spectra of s-polarized wave for a 5 period Si/Air/Si structure with layer thicknesses 100/425/100 µm at angles of incidence equal to 64°, 69°, 74° and 80°. Maximum and minimum transmissivities are 1.837×10^{-3} and 1.157×10^{-7}, respectively.

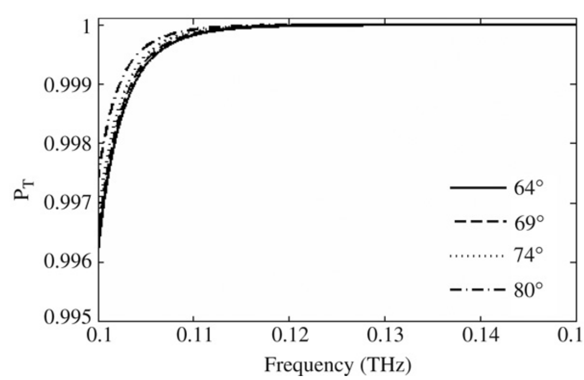

Fig. 3. Degree of polarization (P_T) of light transmitted through a 5 period Si/Air/Si structure with layer thicknesses 100/425/100 µm. Incident angles are 64°, 69°, 74° and 80°. Maximum and minimum values of P_T are 0.9999 and 0.9963, respectively.

In transmission, the extinction ratio, which is defined as the ratio of the desired to the unwanted polarized light, is given by

$$(E.R.)_T = \frac{T_P}{T_S}$$

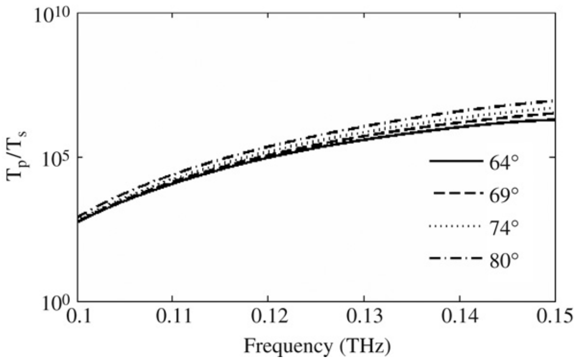

Fig. 4. Extinction ratio $(E.R.)_T$ of light transmitted through a 5 period Si/Air/Si structure with layer thicknesses 100/425/100 μm. Incident angles are 64°, 69°, 74° and 80°. Maximum and minimum values of $(E.R.)_T$ are 8.457×10^6 and 5.322×10^2, respectively.

$(E.R.)_T$ varies between a minimum of 5.322×10^2 and a maximum of 8.457×10^6 (Fig. 4). Thus a high extinction ratio is achieved.

The angular field of the device is 16°, and the effective frequency range is 0.10–0.15 THz.

In reflection, the degree of polarization is defined by [8]

$$P_R = \left|\frac{R_P - R_S}{R_P + R_S}\right|$$

where R_P and R_S are the reflectances for p- and s-polarized light, respectively. The maximum and minimum values of P_R for the range of frequencies and angles investigated were calculated to be equal to 0.9999 and 0.7636, respectively.

The extinction ratio in reflection, defined by

$$(E.R.)_R = \frac{R_S}{R_P}$$

varies between a minimum of 7.462 and a maximum of 4.857×10^7.

Comparison of the results obtained for reflected light with the corresponding ones obtained for transmitted light reveal that the performance of the polarizer is better in transmission. To the best of our knowledge, a wide angle broadband plate polarizer with a high degree of polarization has not been reported before.

4. Conclusion

A wide angle broadband plate polarizer with an angular field of 16° and operating over a frequency range extending from 0.10 THz to 0.15 THz is proposed. The THz frequency region has become an important domain in spectroscopy, imaging and particularly in systems using polarizers and polarizing beam splitters. The proposed polarizer has a high performance in transmission, with maximum and minimum values of the degree of polarization given by 0.9999 and 0.9963, respectively. The extinction ratio varies between a minimum of 5.322×10^2 and a maximum of 8.457×10^6 in transmitted light. The angular field of the polarizer can be increased, but with a reduction in the frequency range of operation.

The polarizer is composed of alternate layers of silicon and air, with a total of eleven layers. Wide angle cube polarizers investigated earlier, have a much larger number of thin film layers cemented between the two prisms constituting a glass cube. As such, the fabrication process of cube polarizers is costly. Moreover, prisms exhibit stress related birefringence, which causes problems in imaging projectors. The proposed polarizer is free from such effects.

Acknowledgements

The authors are grateful to Dr. R. N. Singh, Dr. L. M. Bali and Dr. Sameer Bali for useful discussions related to this work. Thanks are also extended to Dr. N. Malaviya for discussions during the revision of the manuscript.

References

[1] http://www.thznetwork.org/wordpress/index.php/archives/443.
[2] H. Makabe, Y. Hirota, M. Tani, M. Hangyo, Opt. Exp. 15 (2007) 11650.
[3] E. C-Camus, J. L-Hughes, L. Fu, H.H. Tan, C. Jagadish, M.B. Johnston, Opt. Exp. 15 (2007) 7047.
[4] Y. Hirota, R. Hattori, M. Tani, M. Hangyo, Opt. Exp. 14 (2006) 4486.
[5] J-B. Masson, G. Gallot, Opt. Lett. 31 (2006) 265.
[6] E. C-Camus, J. L-Hughes, M.B. Johnston, M.D. Fraser, H.H. Tan, C. Jagadish, Appl. Phys. Lett. 86 (2005) 254102.
[7] J. Xu, G.J. Ramian, J.F. Galan, P.G. Savvidis, A.M. Scopatz, R.R. Birge, S.J. Allen, K.W. Plaxco, Astrobiology 3 (2003) 489.
[8] Li Li, J.A. Dobrowolski, Appl. Optim. 35 (1996) 2221.
[9] M. Thomsen, Z.L. Wu, Appl. Optim. 36 (1997) 307.
[10] J.C. Monga, J. Modern Opt. 36 (1989) 769.
[11] S.M. MacNeille, U. S. patent 2 (403) (1946) 731.
[12] J. Mouchart, J. Begel, E. Duda, Appl. Optim. 28 (1989) 2847.
[13] Li Li, J.A. Dobrowolski, Appl. Optim. 39 (2000) 2754.
[14] Li Li, Opt. Photonicsnews 24 (2003).
[15] I. Hodgkinson, Q.H. Wu, M. Arnold, L. De Silva, G. Beydaghyan, K. Kaminska, K. Robbie, Appl. Optim. 45 (2006) 1563.
[16] T.W. Du Bosq, A.V. Muravjov, R.E. Peale, C.J. Fredricksen, Appl. Optim. 44 (2005) 7191.
[17] M. Born, E. Wolf, Principles of Optics, Cambridge Univ. Press, UK, 1980, p. 1.
[18] P. Yeh, Optical Waves in Layered Media, Wiley, New York, 1998, p. 118.
[19] http://luxpop.com/.